Urania
Jurnal Ilmiah Daur Bahan Bakar Nuklir

Beranda jurnal: https://ejournal.brin.go.id/urania

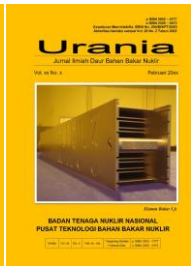

TRANSIENT ACTIVATION ENCAPSULATION ENABLES SEPARATION–FREE PRODUCTION OF HIGHT–PURITY ^{177}Lu IN THE G.A. SIWABESSY MEDIUM–FLUX RESEARCH REACTOR

Maskur [1,2], Yono Sugiharto[3], Endang Sarmini[3], Fransiska Christydira Sekaringtyas[2], Sulaiman[2], Aulia Arivin Billah[2], Lira Aprilia Pujianti[3], Fani Triyatna[3], Rien Ritawidya[2], Muhammad Ridwan[1]*

[1]Department of Chemistry, Faculty of Mathematics and Natural Sciences, Universitas Indonesia
Depok, Jawa Barat, Indonesia 16424
[2]Research Center for Radioisotope, Radiopharmaceuticals, and Biodosimetry Technology – BRIN
Kawasan Sains dan Teknologi B.J. Habibie, Bld. 720, Tangerang Selatan, Banten 15314
[3]Directorate of Nuclear Facility Management – BRIN
Kawasan Sains dan Teknologi B.J. Habibie, Bld. 30, Tangerang Selatan, Banten 15314
*e-mail: muhammad.ridwan@sci.ui.ac.id; mask001@brin.go.id

(Submitted: 03–11–2025, Revised: 29–11–2025, Accepted: 10–12–2025)

ABSTRACT

TRANSIENT ACTIVATION ENCAPSULATION ENABLES SEPARATION – FREE PRODUCTION OF HIGHT – PURITY ^{177}Lu IN THE G.A. SIWABESSY MEDIUM – FLUX RESEARCH REACTOR.

The production of high-purity ^{177}Lu via the direct (n,γ) route is highly dependent not only on isotopic enrichment of the target material but also on the strategic selection of encapsulation materials to reduce radionuclidic impurities. In order to optimize the production of high-specific-activity $^{177}LuCl_3$, this work combines a double-layer containment system consisting of quartz ampoules (SiO_2) and high-purity aluminum capsules (Al 1070) with an enriched Lu_2O_3 target (74% ^{176}Lu). Irradiation was performed in the RSG-GA Siwabessy reactor (BRIN, Indonesia) at a thermal neutron flux of 2 × 10^{14} n·cm^{-2}·s^{-1} for 99 and 193 hours. The target was dissolved in HCl/H_2O_2 to form $^{177}LuCl_3$ and then characterized for radionuclidic purity using high-resolution gamma spectrometry (HPGe) at 48 hours post-end of irradiation (EOI). The results exhibit that this integrated system produces products without detectable container-derived radionuclidic impurities at 48 h post-EOI: activation products from the quartz (^{19}O, T½ = 26.47 s; ^{31}Si, T½ = 2.62 h) and aluminum (^{28}Al, T½ = 2.24 min) containers decayed completely within 24 hours. Under normal HPGe conditions, the metastable isomer ^{177m}Lu (T½ = 160.4 d, σ = 2.85 barn), the sole co-produced radionuclidic species, is present at <1% of total activity at EOI, is not detected spectroscopically from initial state of ^{177}Lu, which can be clinically negligible during the typical therapeutic window (1–14 days post-production). The specific activity obtained was 11 718 mCi/mg (CV = 5.9%) after 193 hours of irradiation, a level adequate for effective radiolabeling of monoclonal antibodies and peptides in targeted radionuclide therapy, despite the presence of stable Lu carrier. This study demonstrates that the interaction between target chemistry and container physics, rather than irradiation parameters alone, is a critical determinant in producing pharmaceutical-grade ^{177}Lu that meets international radionuclidic purity standards (>99.9%). This approach provides a scalable, separation-free production model applicable to medium-flux research reactors globally.

Keywords: Lutetium-177; direct production; encapsulation; radionuclidic purity; separation-free.

INTRODUCTION

Lutetium-177 (^{177}Lu) has emerged as a main radionuclide in the emerging field of targeted radionuclide therapy, particularly within the theranostic framework integrating molecular imaging with precision medicine [1],[2],[3]. The characteristics include a half-life of 6.647 days [1],[4],[5], medium-energy beta$^-$ emission ($E\beta^-$,max = 497 keV) for localized tumor irradiation with an average penetration distance of 1.6 mm and a maximum of 2 mm [6],[7],[8], and co-emitted gamma photons at 112.9 keV and 208.4 keV for single-photon emission computed tomography (SPECT), which provide a remarkable balance between therapeutic efficacy and diagnostic capability [9],[10],[11]. This unique characteristics have led to be extensively used in the treatment of metastatic castration-resistant prostate cancer (via PSMA-targeting agents), neuroendocrine tumors (using somatostatin receptor analogues), and CD20-positive lymphomas [12],[13],[14]. A number of ^{177}Lu-based radiopharmaceuticals have been approved by the U.S. Food and Drug Administration (FDA) and the European Medicines Agency (EMA) resulting in increased global demand for Lu [8],[15],[16][17],[18].

^{177}Lu is primarily produced via two different nuclear routes: (i) the indirect route, which involves neutron irradiation of enriched ^{176}Yb to produce ^{177}Yb, followed by its beta decay to ^{177}Lu, which requires complex post-irradiation radiochemical separation to isolate Lu from the Yb matrix; and (ii) the direct route, which utilizes the ^{176}Lu(n,γ)^{177}Lu reaction on an isotopically enriched lutetium target to produce ^{177}Lu [19],[20][21],[22]. Although the latter does not require chemical separation, ^{177}Lu is produced in the presence of stable lutetium isotopes (carrier), while carrier-free ^{177}Lu is provided by indirect method [15],[23],[24],[25]. The direct route even in the presence of a carrier, however, remains highly attractive for clinical production due to a simple process, potential for high radionuclide purity, and the ability to achieve high specific activity as a critical parameter for efficient radiolabeling of biomolecules with limited binding sites, such as monoclonal antibodies and small peptides [11],[26].

Moreover, neutron flux and duration of irradiation are not the only factors that affect the effectiveness of direct route method. This depends heavily on two common-overlooked technical factors, including (1) the chemical form and isotopic composition of the target material, and (2) the elemental composition and structural design of the target encapsulation system (ampoule and capsule) [24],[27],[28]. Though the majority of literature focuses on optimizing irradiation parameters, only a few studies have investigated on how the synergistic interaction between the target chemical matrix (e.g., oxide, metal, or salt) and the encapsulation materials (e.g., quartz, aluminum, or stainless steel) regulate the final radionuclide purity of the product [24],[29],[30]. This is an important factor because the encapsulation materials act a mechanical barrier and are susceptible to neutron activation. If the constituent isotopes have significant activation cross-sections, this may result in radionuclidic impurities that compromise the purity, safety, and regulatory compliance of the final product $^{177}LuCl_3$ [31],[32].

The novelty of this work is the use of a comprehensive, materials-focused strategy to optimize the direct production of ^{177}Lu. This work demonstrates that the strategic combination of an isotopically enriched Lu_2O_3 target (74% ^{176}Lu) with a double-layer containment system, comprising a chemically inert quartz (SiO_2) ampoule and high-purity aluminum (Al 1070) inner/outer capsules, is a main factor in achieving undetectable radionuclidic impurities at 48 h post-end-of-irradiation (EOI), a standard timepoint for clinical quality control. Quantitative results of nuclear activation routes of each system component showed that potential impurities from the targets (e.g., ^{177m}Lu, ^{19}O), and ampoule and capsules (e.g., ^{31}Si, ^{28}Al) decayed completely within 24 hours or were formed in clinically negligible amounts [33]. It is important to note that this study exhibits that a specific activity exceeding 11,000 mCi/mg is sufficient for high-efficiency antibody radiolabeling, which can be achieved in the presence of a carrier considering adequately enriched targets and optimized irradiation times, as supported by established saturation models [23],[34],[35].

This research was performed at the G.A. Siwabessy Multipurpose Reactor (RSG-GA Siwabessy), BRIN, Indonesia, operating at a thermal neutron flux of

 DOI: https://doi.org/10.55981/urania.2026.13640

2×10^{14} n·cm^{-2}·s^{-1}. The results reported here have a big practical implications as it provides a reproducible, separation-free, and financially feasible production framework for medium-flux research reactors globally, enabling a consistent supply of pharmaceutical-grade ^{177}Lu for clinical application development [36],[37].

METHODOLOGY

Materials and Equipment

The materials used in this study consisted of 74% ^{176}Lu-enriched Lu_2O_3 (Isoflex, USA), hydrochloric acid (HCl, Merck, Germany), hydrogen peroxide (H_2O_2, Merck, Germany), quartz ampoules, and inner/outer capsules fabricated from high-purity aluminum (Al 1070, Indonesia). The equipment used includes the G.A. Siwabessy nuclear reactor (BRIN, Indonesia), a hot cell, Pyrex glassware (Germany), a high-purity germanium (HPGe) gamma spectrometer (Mobius, USA), and a dose calibrator (Comecer, Italy).

Production of Lutetium-177

^{177}Lu was produced via the direct neutron activation route. The production process began with the preparation of the target: 0.29-0.50 mg of 74% ^{176}Lu-enriched Lu_2O_3 was weighed and loaded into a quartz ampoule, which was subsequently sealed by welding. The sealed ampoule was then placed inside an inner aluminum capsule, which was capped and welded shut. A leak test was performed to ensure integrity of the container. Shortly after ensuring there were no leaks, the inner capsule was inserted into an outer aluminum capsule. A swab test was conducted to verify that the outer capsule is free from radioactive contamination. Once confirmed, the encapsulated target was ready to be irradiated in the G.A. Siwabessy reactor for 99 and 193 hours.

Post-irradiation, the radioactive capsule (containing activated ^{177}Lu) was transferred to a hot cell for further processing. The irradiated target material was transferred to a beaker glass and then completely dissolved by adding 2 mL of 6N HCl. After that, 2 mL of H_2O_2 was added, and the mixture was then stirred and heated to nearly dryness (without boiling). After drying, 3 mL of 0.05M HCl was added and stirred for 5 minutes to form the final product $^{177}LuCl_3$. The radionuclide purity was characterized by gamma spectrometry, and the radioactivity was measured using an ionization chamber:

RESULTS AND DISCUSSION

Selection of target material and the materials used for the ampoule and inner/outer capsules hold a significant impact on the quality of ^{177}Lu produced by neutron irradiation in the direct route. In this study, 74% ^{176}Lu-enriched Lu_2O_3 was used as the target. In order to elucidate of target chemical form and isotopic enrichment, the physical and nuclear properties of Lu_2O_3 are summarised in Table 1. Comprehensive study of these parameters is essential, as they have a direct impact on neutron activation efficiency, product radionuclidic purity, and irradiation safety.

Table 1. Physical and nuclear properties of Lu_2O_3 target material.

Property	Value/ Isotope	Abbundance (%)	Cross section (barn)	Product radioisotope	Half-life
Melting point	2490 °C	-	-	-	-
Lutetium isotopes	^{175}Lu	97.4	7	^{176}Lu	stable
	^{176}Lu	2.6	2100	^{177}Lu	6.647 days
			2.85	^{177m}Lu	160.4 days
Oxygen isotopes	^{16}O	99.74	0.00019	^{17}O	stable
	^{17}O	0.04	0.24	^{18}O	stable
	^{18}O	0.22	0.00016	^{19}O	26.47 seconds

Due to the extremely high melting point of 2490°C, Lu_2O_3 is ideal for irradiation inside nuclear reactor cores, where energy deposition from neutron flux and gamma radiation may generate local temperatures surrounding the target to rise noticeably. This excellent thermal stability ensures that the target remains solid and does not melt or deform during the 193-hour irradiation period. Moreover, it also contributes to secure

operational safety integrity by preventing mechanical failure of the quartz ampoule and potential leakage of radioactive material into the reactor cooling system.

It can be observed from Table 1 that ^{175}Lu dominated at 97.4% of the natural isotopic abundance of lutetium, while ^{176}Lu only existed at 2.6%. Neutron irradiation of natural Lu without enrichment would primarily produce stable ^{176}Lu (via the ^{175}Lu(n,γ)^{176}Lu reaction) and only a small amount of the desired ^{177}Lu (via ^{176}Lu(n,γ)^{177}Lu). In this study, the use of Lu_2O_3 enriched to 74% ^{176}Lu is a strategic approach to enhance the production yield of ^{177}Lu. The possibility of the desired (n,γ) reaction was substantially enhanced by increasing the target isotope fraction (^{176}Lu). This study resulted specific activity of ^{177}Lu sufficient for theranostic radiolabeling, which requires a very high activity-to-ligand mass ratio.

Furthermore, the thermal neutron cross-section (σ) is the most critical nuclear parameter that determines the rate of radionuclide production. It can be observed from Table 1 that ^{176}Lu had a very large cross-section of 2100 barns for the (n,γ) reaction that produces ^{177}Lu, compared to ^{175}Lu which only had a cross-section of 7 barns. This significant difference (more than 300-fold) indicated that the contribution ^{176}Lu to ^{177}Lu production was dominant due to its high reaction efficiency, though the limited natural abundance. Therefore, enrichment of the ^{176}Lu isotope increased markedly the production yield of ^{177}Lu.

The cross-section for the formation of the metastable isomer ^{177m}Lu (2.85 barns), is also displayed in Table 1. Although this value was significantly smaller than that of ^{177}Lu, a potential presence of ^{177m}Lu as an impurity should be taken into account due to the long half-life (160.4 days). However, the production ratio is relatively small (approximately 0.1-1%) compared to ^{177}Lu, thus it is not significant for short-term clinical applications.

In addition, Table 1 revealed that the final product could be contaminated by radionuclides generated from oxygen isotopes in Lu_2O_3. It has been widely known that ^{177}Lu (T½ = 6.647 days) has an ideal beta and gamma emissions for therapy and imaging. For clinical applications, ^{177}Lu will be used within 1-2 weeks post-production, and the dosimetry contribution from metastable impurity of ^{177m}Lu (T½ = 160.4 days) is negligible as it is produced in a relatively small fraction. Moreover, the oxygen isotopes (^{16}O, ^{17}O, ^{18}O) in Lu_2O_3 could be activated by neutrons. The ^{18}O(n,γ)^{19}O reaction produced the radionuclide ^{19}O with a very short half-life (26.47 seconds) which did not influence the purity of the product purity as it decayed completely within minutes post-irradiation and was not detected in purity testing at 48 hours after EOI.

The comprehensive analysis explained above provides a rationale that 74% ^{176}Lu-enriched Lu_2O_3 is the optimal target material for direct production of ^{177}Lu. The combination of physical (high melting point) and nuclear properties (large cross-section of ^{176}Lu) makes it ideal to obtain a product with high specific activity and excellent radionuclidic purity.

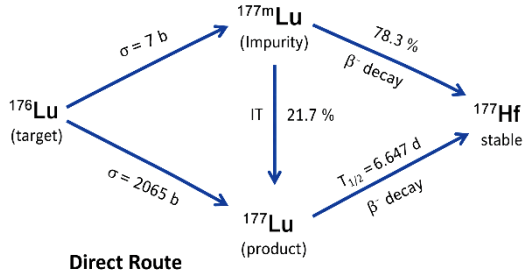

Figure 1. Reaction scheme of ^{177}Lu Production via direct route

The primary nuclear mechanism during neutron irradiation of 74% ^{176}Lu-enriched Lu_2O_3 target in a nuclear reactor is illustrated in Figure 1. This scheme not only describes the synthesis route of ^{177}Lu but also depicts the potential formation of the metastable isomer of ^{177m}Lu, which is a radionuclidic impurity that needs to be considered in the direct route.

The process initiated with the ^{176}Lu nucleus (enriched target isotope) capturing a thermal neutron (an (n,γ) reaction) resulted in the formation of an excited ^{177}Lu compound nucleus. This excited nucleus was unstable and rapidly decompose to the initial state by emitting gamma rays. The majority (>99%) of this excited nucleus decayed immediately to the initial state of ^{177}Lu with a 6.647-day half-life and emitted therapeutic beta particles and diagnostic gamma rays.

 DOI: https://doi.org/10.55981/urania.2026.13640

On the other hand, there was a minor pathway, ^{177m}Lu, in which the excited nucleus was captured in a metastable state instead of transiting to the initial state. This metastable state was an isolated energy level at 160.6 keV above the initial state, with a considerably longer half-life of 160.4 days. ^{177m}Lu was generated through an indirect nuclear transition with a small fraction of about 0.1–1% of the total ^{177}Lu production, as supported by the cross-section data mentioned in Table 1 (σ = 2.85 barn for ^{177m}Lu vs. 2100 barn for ^{177}Lu).

Furthermore, the direct route has a major advantage in that post-irradiation radiochemical separation is not required, as there is no main isotope or chemical impurities, such as Yb from the indirect method. In addition, the final product, $^{177}LuCl_3$, is obtained directly through target dissolution which could reduce the risk of cross-contamination and loss of activity.

Besides the target material, the selection of the target encapsulation (e.g., ampoule, inner and outer capsules) had a significant impact on the quality of the final product ^{177}Lu. The materials used in this study are described in Table 2.

Table 2. Characteristics of the ampoule, inner, and outer capsules used in the production of ^{177}Lu

Component	Material Composition	Melting Point (°C)	Isotope abundance (%)	Cross section (barn)	Radioisotope Product	Half life
Inner/outer capsule	Al (Al 1070)	660.3	^{27}Al (100%)	0.231	^{28}Al	2.24 min
Ampoule	Quartz (SiO_2)	1715	^{28}Si (92,2%)	0.169	^{29}Si	stable
			^{29}Si (4,7%)	0.119	^{30}Si	stable
			^{30}Si (3,1%)	0.107	^{31}Si	2.62 min
			^{16}O (99.74%)	0.00019	^{17}O	Stable
			^{17}O (0.04%)	0.235	^{18}O	Stable

.

The selection of these materials had significant impact on the purity of radionuclidic, the integrity of irradiation safety, and the feasibility of production. Quartz ampoule (SiO_2) acts as the primary container for Lu_2O_3, effectively preventing direct contact between the target and the reactor coolant water, thus reducing cross-contamination. As the quartz is non-porous and chemically inert, it also mitigates the risk of radioactive material being released to the reactor environment in the case of mechanical failure and ensures that Lu is not absorbed into the container matrix. Moreover, SiO_2 contains stable isotopes, ^{28}Si (92.2%), ^{29}Si (4.7%), ^{30}Si (3.1%), ^{16}O(99.74%), ^{17}O (0.04%), and ^{18}O (0.22%), which provide the beneficial effect of producing impurity radionuclides with a very short half-life; ^{31}Si (T½ = 2.62 hours) from ^{30}Si activation (σ = 0.107 barn) and ^{19}O (T½ = 26.47 seconds) from ^{18}O activation (σ = 0.00018 barn), both of them decay completely within a few hours post-irradiation. It can be observed in Table 2 that the quartz had a very small cross-section (< 0.24 barn), which suggested that the intrinsic activity of these impurities was low. Therefore, quartz ampoules are not only a technical solution but also allow for a physical barrier without affecting product purity.

Furthermore, the inner and outer capsules were composed of high-purity aluminum (Al 1070, purity >99.7%), working as a secondary barrier against contamination. These capsules perform by protecting the quartz ampoule from mechanical stress and turbulence in the reactor pool, reducing surface contamination of the ampoule from radioactive particulates in the water pool, and facilitating handling and transportation of the target before and after irradiation. In addition, the use of high-purity aluminum is essential to circumvent the activation of trace impurities (e.g., Fe, Cu, or Zn), which could have large cross-sections and long half-life, thus reduce product purity and increase the radiation dose to the operator.

The combination of quartz ampoules and aluminum capsules creates an ideal multi-layer containment system. The chemical and radionuclidic purity of the product is ensured by the first layer (quartz), while operational safety and rapid decontamination are provided by the second layer (aluminum). This system effectively

minimizes the formation of radionuclidic impurities with a long half-life, which has been known that all potential radionuclidic impurities (^{19}O, ^{31}Si, ^{28}Al) decay completely within 24 hours. Moreover, the melting points of quartz (1715 °C) and aluminum (660.3 °C) which were above the maximum operational temperature in the RSG-GA Siwabessy reactor core for 193 hours of irradiation, ensure the stability of the structure and prevent thermal failure. During heating and cooling cycles, the compatible thermal expansion coefficients of Lu_2O_3, SiO_2, and Al contribute to prevent cracking or leakage induced by thermal stress.

Table 3. ^{177}Lu production data at the G.A. Siwabessy Reactor, BRIN, Indonesia, using a 74% ^{176}Lu-enriched Lu_2O_3 target in various irradiation times and target masses

Irradiation Time (hour)	Target mass (mg)	Activity (mCi)	Specific activity (mCi/mg)	Average specific activity (mCi/mg)
193	0.50	5535	11070.0	11718.4 mCi/mg (CV=±5.9%)
	0.45	5137	11415.6	
	0.33	4181	12669.7	
99	0.47	2957	6291.5	6066.3 mCi/mg (CV= ±4.9%)
	0.29	1662	5731.0	
	0.33	2100	6176.5	

The data in Table 3 not only described the yield of production but also exhibited critical indicators in terms of process efficiency, optimisation of irradiation parameter, and clinical compatibility of the final product. It can be observed in Table 3 that the average specific activity increased remarkably from 6066.3 mCi/mg (CV=±4.9%) to 11718.4 mCi/mg (CV=±5.9%) when the irradiation time was extended from 99 to 193, which was approximately doubled the product yield. This phenomenon was in line with the basic principles of neutron activation reports that the final activity increased to saturation activity as the irradiation time increased.

In theory, the maximum activity in neutron irradiation is determined by the number of target atoms, the abundance of target isotope, neutron cross-section, neutron flux, irradiation time, and the half-life of radionuclide. Considering the half-life of ^{177}Lu of 6.647 days (~161 h), a 99 h of irradiation (~0.6 × T½) achieved ca. 45%, while a 193 h of irradiation (~1.2 × T½) reached ca. 70% of saturation activity. These results demonstrated that there was a significant increase in specific activity as increasing irradiation time, which agrees with the exponential decay model and existing literature [29].

In terms of specificity, high specific activity (>10,000 mCi/mg) of radiopharmaceuticals is essential for theranostic applications using antibodies or peptides. Monoclonal antibodies (e.g., rituximab, PSMA, trastuzumab, ofatumumab) and peptides have a limited number of binding sites. If the specific activity is low, a larger mass of ligand is required to deliver a sufficient therapeutic dose that potentially leading to immunological side effects or non-specific receptor saturation. The $^{177}LuCl_3$ produced in this study had a specific activity more than 11,000 mCi/mg after 193 h of irradiation, proving ideal for advance clinical applications which include radiolabeling of antibodies with an optimal activity-to-mass ratio. This phenomenon complies to the international pharmacopeia standards and the recommendations of EANM/SNMMI for radioligand therapy [6].

Though 193 h of irradiation resulted in higher specific activity, economic efficiency and reactor capacity would remain be crucial factors. On the other hand, irradiation for 99 h generated a specific activity of ~6,000 mCi/mg, which is still suitable for numerous preclinical or therapeutic applications using ligands with high binding capacity, such as small peptides. Hence, it is possible to maintain cost and product quality by optimising irradiation times based on application needs. The increase in specific activity is not associated with a decline of radionuclidic purity, as the containment system (quartz ampoules and Al capsules) has been proven to be highly effective in

 DOI: https://doi.org/10.55981/urania.2026.13640

limiting the formation of impurities. This approach allows optimal utilization of reactor resources without affecting product quality.

The data in Table 3 also demonstrated a good reproducibility. In this study, three replication were performed with various target masses (0.33–0.50 mg for 193 h and 0.29–0.47 mg for 99 h). The relatively small of coefficient of variation (CV) (5.9% for 193 h and 4.9% for 99 h) indicated that the production process, from target preparation and irradiation to post-irradiation dissolution, was stable and well-controlled. This parameter acts as a critical indicator for scalability and quality control in routine production.

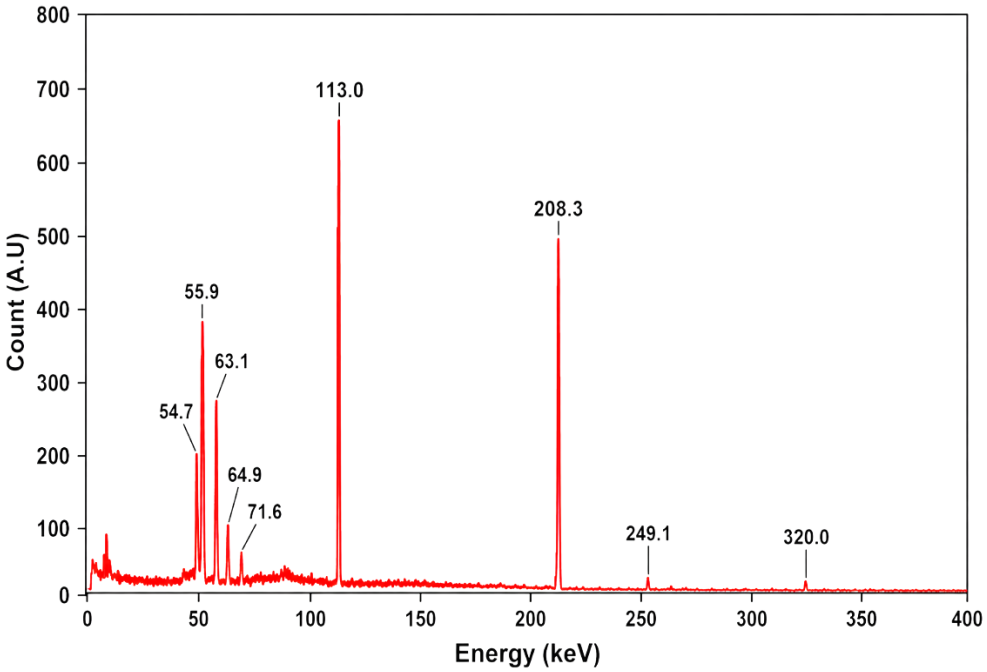

Figure 2. The gamma-ray spectrum of ^{177}Lu obtained from the HPGe detector

The gamma-ray emission spectrum of $^{177}LuCl_3$ measured using a High-Purity Germanium (HPGe) gamma spectrometer at 48 hours post-end-of-irradiation (EOI) is depicted in Figure 2. This spectrum provided a scientific evidence of the hypothesis that there was no radionuclidic impurities detected at 48 h post-EOI, as determined by the limit of detection (LoD) of the HPGe system under the acquisition conditions. From Figure 2 it can be seen that there were nine energy peaks, which all of them fulfill the decay profile of ^{177}Lu defined by the Bureau International des Poids et Mesures (BIPM) and standard nuclear data references [38]. The first four peaks (54.7, 55.9, 63.1, and 64.9 keV) were characteristic X-rays of lanthanides, generated through internal conversion and secondary electron capture from the excited ^{177}Lu nucleus. Those peaks are generally found in elements with high atomic numbers (Z = 71) and work as supplementary markers for radionuclide identification. The last five peaks (71.6, 113.0, 208.3, 249.1, and 320.0 keV) were direct gamma transitions from the ^{177}Lu nucleus to the initial state. Among those peaks, the peak of 208.3 keV (11.0% intensity) is the primary emission used for SPECT imaging, while the 113.0 keV peak (6.4% intensity) is generally employed to quantify the activity and validation.

Moreover, there were no additional gamma peaks resulting from radionuclidic impurities that observed above background level, such as 197 keV or 1357 keV from ^{19}O, 657 keV from ^{31}Si, or 1779 keV from ^{28}Al. This absence is consistent with the predicted decay characteristic of container-derived activation products (Figure 4). All of these products had a half-life of ≤ 2.62 h, which suggests that they would decay to undetectable levels before the measurement timepoint of 48 hours.

The potential contribution of the metastable isomer ^{177m}Lu (T½ = 160.4 d) was unable to be distinguished spectroscopically using standard HPGe conditions, as its primary gamma emission at 208.6 keV almost completely overlaps with the 208.3 keV peak of initial state ^{177}Lu. However, based on cross-sectional data (σ = 2.85 barn for ^{177m}Lu vs. 2100 barn for ^{177}Lu) and current literature, the fractional abundance at EOI is estimated to be less than 1% and remains clinically negligible during the unique therapeutic window (1–14 days post-production). Even though ^{177m}Lu is technically a radionuclidic impurity, it is undetected as a separate element in gamma spectrometry at 48 h, and its presence does not contradict the pharmacopeial requirements for radionuclidic purity (>99.9% ^{177}Lu). The obtained purity meets the high standards defined by international pharmacopeias, such as USP 825 and the European Pharmacopeia monograph for $^{177}LuCl_3$, thereby ensuring precise dosimetry, patient safety, and compliance with regulatory standards for clinical applications.

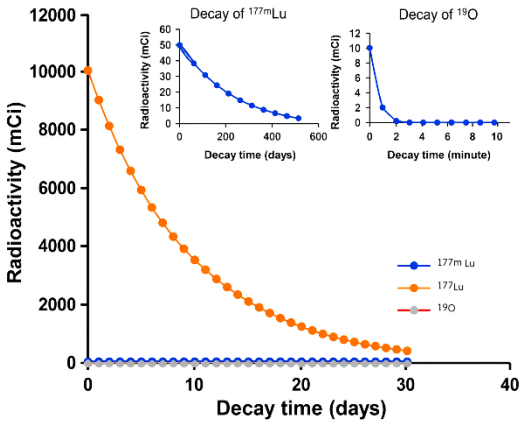

Figure 3. Theoretical decay curves for ^{177}Lu, ^{177m}Lu, and ^{19}O produced from Lu_2O_3 target.

Figure 3 illustrates the theoretical decay curves for the primary radionuclide (^{177}Lu) and the potential impurity radionuclides (^{177m}Lu and ^{19}O) generated during neutron irradiation of the 74% ^{176}Lu-enriched Lu_2O_3 target. This graph provides quantitative evidence confirming the statement of no detectable radionuclidic impurities at 48 h post-EOI, which is the standard timepoint for clinical quality control and gamma spectrometric analysis.

It can be observed form Figure 3 that the activity of ^{177}Lu (blue line, T½ = 6.647 days) was significantly greater than ^{177m}Lu (red line, T½ = 160.4 days). This result was in line with the cross-section data mentioned in Table 1, where the ^{176}Lu(n,γ)^{177}Lu reaction had a noticeable higher in σ of 2100 barns (ca. 700-fold) compared to the ^{177m}Lu with 2.85 barns. Therefore, the initial fraction of ^{177m}Lu at EOI was only about 0.1–1% of the total ^{177}Lu activity, as reported by Pillai et al. (2003) and Dash et al. (2015) [36].

Despite having a longer half-life, the contribution of ^{177m}Lu to the total dose during a typical clinical application period (generally 1–14 days post-EOI) is very limited. On the 7th day of post-production, for instance, the activity of ^{177}Lu decreased to ca. 50% from initial value, while the activity of ^{177m}Lu declined by less than 5%. Still, as the initial fraction was only 0.5%, the contribution to the total activity remained <1%. The means that radiation dose received by the patient comes entirely from pure ^{177}Lu, without significant influence from impurities with a longer half-life. This parameter meets the international pharmacopeial standards (USP 825, Ph. Eur.), which require radionuclidic purity of >99.9% for therapeutic applications.

The absence of container-derived contamination is shown by the ^{19}O curve (green line, T½ = 26.47 seconds) that decayed completely within a few minutes post-EOI. The graph exhibited that though the oxygen atoms in the Lu_2O_3 target and the SiO_2 ampoule were activated by neutrons (via the ^{18}O(n,γ)^{19}O reaction), their very short half-life ensured that ^{19}O had decayed completely by the time measurements were performed at 24 - 48 hours post-EOI. This phenomenon strengthens the statements presented in Table 2 and Figure 4, where all radionuclide impurities of the containment materials (^{19}O, ^{31}Si, ^{28}Al) have a very short half-life and decay completely before characterization is performed.

Theoretical decay kinetics of radionuclide impurities generated from neutron activation of the containment materials, ^{31}Si and ^{19}O from the quartz ampoule (SiO_2) and ^{28}Al from the aluminum capsules (Al 1070), during the ^{177}Lu production process are displayed in Figure 4.

 DOI: https://doi.org/10.55981/urania.2026.13640

This graph provides quantitative and predictive evidence supporting the main claim that the combination of quartz ampoule and high-purity aluminum capsules could effectively guarantee no detectable radionuclidic impurities at 48 h post-EOI, which is the standard timepoint for clinical quality control and gamma spectrometry characterization.

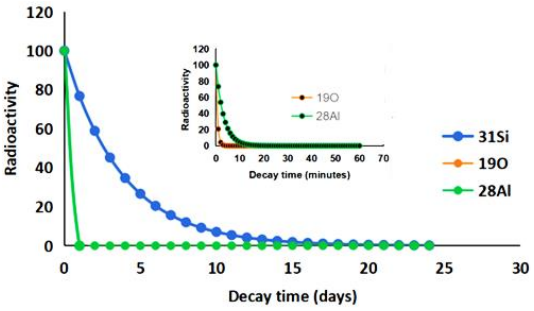

Figure 4. Theoretical decay curves for ^{31}Si, ^{19}O, and ^{28}Al produced from the quartz ampoule and aluminum capsules.

In terms of decay rate, there are three potential radionuclide impurities from the containment materials that have a very short half-life, including ^{19}O (T½ = 26.47 sec) which decay completely within minutes, ^{28}Al (T½ = 2.24 min) which decay to <0.1% of the initial activity in 30 min, and ^{31}Si (T½ = 2.62 h) which decay by >99% in 20 hours. It can be observed in Figure 4 that the activity of all three radionuclides was nearly unnoticed at 24 hours post-production, which occurred before the gamma spectroscopy measurement at 48 hours (Figure 2). This phenomenon explains the reason behind the final spectrum did not exhibit any gamma peaks from ^{19}O (197 keV, 1357 keV), ^{31}Si (657 keV), or ^{28}Al (1779 keV), as they had completely decayed before the measurement. Moreover, the formation of these radionuclide impurities could be predicted based on the nuclear data mentinoned in Table 2, such as ^{19}O is produced from the activation of ^{18}O (abundance 0.22%, σ = 0.00018 barn) in SiO_2, ^{31}Si is generated from the activation of ^{30}Si (abundance 3.1%, σ = 0.107 barn) in SiO_2, and ^{28}Al is obtained from the activation of ^{27}Al (abundance 100%, σ = 0.231 barn) in Al 1070.

Although the isotopes in the containment materials could be activated, the initial activity formed is at a lower extent due to the activation cross-sections is very small (< 0.24 barn). In addition, because of their very short half-life, these isotopes have no effect on radiation contamination or spectroscopic interference at the measurement time point. Overall, Figure 4 validated the experimental design, particularly the selection of post-production measurement time for 48 hours. The time obtained was determined scientifically to ensure the fully decay of all container-derived impurities (^{19}O, ^{28}Al, ^{31}Si), while the activity of ^{177}Lu remained high (>80% of EOI). This result also provides accuracy for radiolabeling and characterization, which normally starts at 24 - 48 hours post-production.

Table 4. Comparison between direct and indirect routes of ^{177}Lu production

Aspects	Research Results	Yang, et al. [39]
Production Method	Direct route nuclear reactor	Indirect route nuclear reactor
Target materials	74% enriched [^{176}Lu]Lu_2O_3	74% enriched [^{176}Yb]Yb_2O_3
Target mass	0.3 mg	300 mg
Separation process	Without separation	Three stages
Total activity	1623-5535 mCi	1900 mCi
Specific activity	11070-12669.7 mCi/mg (193 h of irradiation) 5731-6291.5 mCi/mg (99 h of irradiation)	2976-3745 GBq/mg 80432-101216 mCi/mL
Radioactivity concentration	554-1845 mCi/mg	39-41 GBq/mL 1054-1108 mCi/mL
Radiochemical purity	>99%	>99 %
Radionuclidic purity	>99,99	>99,99 %
Radionuclide impurity	total ^{177m}Lu < 0,01	total ^{175}Yb,^{177m}Lu < 0,01
pH	1	1,5

The production of ^{177}Lu in this work via direct route method was summarised in Table 4. Overall, these results were quite similar to previous study reported by Yuchuan Yang et al. (2023) [39] which employed an indirect route, achieving high radiochemical dan radionuclidic purity. However, a notable difference concerns the specific activity of $^{177}LuCl_3$. It can be observed in Table 4 that the specific activity of $^{177}LuCl_3$ in this study was significantly lower (ca.7-fold) than previous study conducted by Yuchuan Yang et al. (2023). This outcome could be attributed to the use of direct route that produces carrier-added $^{177}LuCl_3$, whilst the previous study utilised an indirect route that yields a non-carrier-added product. These results indicated time-dependent activity, with the longer irradiation times leading to remarkable increases in specific activity. Interestingly, though the direct route showed a lower specific activity, it has been reported to be sufficient to enable efficient radiolabeling of biomolecules, such as monoclonal antibodies [23],[34]. The principal advantage of the direct route is a simpler method compared to the indirect route, as it does not require a post-irradiation radiochemical separation process, thus reducing complexity, production cost, and the potential for activity loss or cross-contamination, while still ensuring compliance with the requirements for pharmaceutical grade ^{177}Lu, including radionuclidic purity (>99,9%) and radiochemical purity (>95%). This makes the optimized direct route a highly practical and scalable approach for application in medium-flux research reactors. On the other hand, this study has not explored extensively some aspects of ^{177}Lu production and in process quality control to produce pharmaceutical grade products. Therefore, further work may be needed to focus on several aspects, including:

a. Enhancement of specific activity using ^{176}Lu targets with higher isotopic enrichment (>95%)
b. Process validation to control the quality of radiopharmaceuticals by conducting in vitro stability tests at room temperature, under storage (at 4°C) and blood plasma at 37°C.
c. Development of comprehensive analytical method validation protocols in accordance with USP <825> and Ph. Eur. guidelines, including sterility test and pyrogenicity test to ensure compliance with GMP standards.

CONCLUSIONS

This study successfully demonstrated that the optimal combination of target chemical form (74% ^{176}Lu-enriched Lu_2O_3) and a double-layer containment system (quartz ampoule + high-purity aluminium capsules) in a direct route in the RSG-GA Siwabessy reactor produced $^{177}LuCl_3$ without detectable radionuclide impurities at 48 h post-EOI and a high specific activity of 11,718.4 mCi/mg (CV = ±5.9%) after 193 hours of irradiation. This success was assisted by the thermal stability of the target, the large reaction cross-section (2100 barn), and the intrinsic nuclear design of the containment system, which minimized and ensured the rapid decay of all potential radionuclide impurities (^{19}O, ^{31}Si, ^{28}Al) within 24 hours, allowing them to remain undetected in the characterization conducted 48 hours post-production. This comprehensive strategy provides an efficient, safe, and scalable production solution for antibody-based theranostic applications, without the need for additional radiochemical separation.

ACKNOWLEDGEMENTS

The authors gratefully acknowledge funding from the National Research and Innovation Agency (BRIN) under the 2022 HITN Research scheme (BRIN Director Decree No. B-528/III.2/TN/12/2022).

REFERENCES

[1]. S. C. George and E. J. J. Samuel, “Developments in 177Lu-based radiopharmaceutical therapy and dosimetry,” Frontiers in Chemistry, vol. 11, pp. 1–13, 2023.
[2]. K. Chakraborty, J. Mondal, J. M. An, J. Park, and Y.-K. Lee, “Advances in radionuclides and radiolabelled peptides for cancer therapeutics,” Pharmaceutics, vol. 15, p. 971, 2023.
[3]. A. Gafita et al., “RECIP 1.0 predicts progression-free survival after [177Lu]Lu-PSMA radiopharmaceutical therapy in patients with metastatic castration-resistant prostate cancer,”

Journal of Nuclear Medicine, vol. 65, pp. 917–922, 2024.

[4]. J. Gawel and Z. Rogulski, “The challenge of single-photon emission computed tomography image segmentation in the internal dosimetry of 177Lu molecular therapies,” Journal of Imaging, vol. 10, pp. 1–23, 2024.

[5]. K. Sjögreen et al., “EANM dosimetry committee recommendations for dosimetry of 177Lu-labelled somatostatin-receptor- and PSMA-targeting ligands,” European Journal of Nuclear Medicine and Molecular Imaging, vol. 49, pp. 1778–1809, 2022.

[6]. [6] J. A. Korsen et al., “Neuroendocrine prostate cancer,” Proceedings of the National Academy of Sciences, vol. 119, pp. 1–7, 2022.

[7]. S. J. Keam, “Lutetium Lu 177 vipivotide tetraxetan: First approval,” Molecular Diagnosis & Therapy, vol. 26, pp. 469–477, 2022.

[8]. T. Ladrière et al., “Safety and therapeutic optimization of lutetium-177 based radiopharmaceuticals,” Pharmaceutics, vol. 15, pp. 1–19, 2023.

[9]. P. E. Harris, K. Zhernosekov, and A. Harris, “The evolution of PRRT for the treatment of neuroendocrine tumors: What comes next?” Frontiers, vol. 13, pp. 1–9, 2022.

[10]. U. Hennrich, “Lutathera®: The first FDA- and EMA-approved radiopharmaceutical for peptide receptor radionuclide therapy,” Pharmaceuticals, vol. 12, pp. 1–8, 2019.

[11]. U. Hennrich and M. Eder, “[177Lu]Lu-PSMA-617 (Pluvicto™): The first FDA-approved radiotherapeutical for treatment of prostate cancer,” Pharmaceuticals, vol. 15, pp. 1–13, 2022.

[12]. B.-N. Park et al., “177Lu anti-angiogenic radioimmunotherapy targeting ATP synthase in gastric cancer model,” Antibodies, vol. 13, p. 51, 2024.

[13]. K. Shim et al., “Cure of disseminated human lymphoma with [177Lu]Lu-ofatumumab in a preclinical model,” Journal of Nuclear Medicine, vol. 64, pp. 542–548, 2023.

[14]. A. Y. Jia et al., “Lutetium-177 DOTATATE: A practical review,” Practical Radiation Oncology, vol. 12, pp. 305–311, 2022.

[15]. S. Sharma and M. K. Pandey, “Radiometals in imaging and therapy: Highlighting two decades of research,” Pharmaceutical Journal, vol. 1460, pp. 1–44, 2023.

[16]. K. Herman et al., “Set up a theranostics center,” Journal of Nuclear Medicine, vol. 63, pp. 1836–1843, 2022.

[17]. R. Garje, T. A. Hope, R. B. Rumble, and R. A. Parikh, “Systemic therapy update on 177Lu-PSMA-617 for metastatic castration-resistant prostate cancer: ASCO guideline rapid recommendation Q and A,” JCO Oncology Practice, vol. 19, pp. 132–135, 2023.

[18]. J. Fallah et al., “FDA approval summary: Lutetium Lu 177 vipivotide tetraxetan for patients with metastatic castration-resistant prostate cancer,” Clinical Cancer Research, vol. 29, pp. 1651–1657, 2023.

[19]. S. W. Ling et al., “Advances in 177Lu-PSMA and 225Ac-PSMA radionuclide therapy for metastatic castration-resistant prostate cancer,” Pharmaceutical Journal, vol. 14, pp. 1–17, 2022.

[20]. L. Shao, “Optimization of deuteron irradiation of 176Yb for producing 177Lu of high specific activity exceeding 3000 GBq/mg,” Molecules, vol. 28, pp. 1–22, 2023.

[21]. S. Patra et al., “Electrochemical separation and purification of no-carrier-added 177Lu for radiopharmaceutical preparation: Translation from bench to bed,” Chemical Engineering Journal Advances, vol. 14, p. 100444, 2023.

[22]. M. Balzer et al., “Evaluation of the 177mLu concentration in in-house produced 177Lu-radiopharmaceuticals and commercially available Lutathera®,” EJNMMI Radiopharmacy and Chemistry, vol. 8, 2023.

[23]. A. Dash, M. R. A. Pillai, and F. F. Knapp, “Production of 177Lu for targeted radionuclide therapy: Available options,” Nuclear Medicine and Molecular Imaging, vol. 49, pp. 85–107, 2015.

[24]. D. Sairanbayev et al., “Analysis of lutetium-177 production at the WWR-K research reactor,” Applied Radiation and Isotopes, vol. 169, p. 109561, 2021.

[25]. K. Tomiyoshi et al., “Optimization processes of clinical chelation-based radiopharmaceuticals for pathway-

directed targeted radionuclide therapy in oncology," Pharmaceuticals, vol. 16, pp. 1–18, 2024.

[26]. M. Lin et al., "Monoclonal antibody based radiopharmaceuticals for imaging and therapy," Current Problems in Cancer, vol. 45, p. 100796, 2021.

[27]. V. S. Le, "Specific radioactivity of neutron induced radioisotopes: Assessment methods and application for medically useful," Molecules, vol. 16, pp. 818–846, 2011.

[28]. R. A. Kuznetsov et al., "Production of lutetium-177: Process aspects," Radiochemistry, vol. 61, pp. 381–395, 2019.

[29]. S. C. Rubel Chakravarty, "A review of advances in the last decade on target cancer therapy using 177Lu: Focusing on 177Lu produced by the direct neutron activation route," Journal of Nuclear Medicine and Molecular Imaging, vol. 11, pp. 443–475, 2021.

[30]. W. V. Vogel, S. C. van der Marck, and M. W. J. Versleijen, "Challenges and future options for the production of lutetium-177," European Journal of Nuclear Medicine and Molecular Imaging, vol. 48, pp. 2329–2335, 2021.

[31]. Z. Talip et al., "A step-by-step guide for the novel radiometal production for medical applications: Case studies," Molecules, vol. 25, pp. 1–29, 2020.

[32]. Y. Nagai et al., "Estimated isotopic compositions of Yb in enriched 176Yb for producing 177Lu with high radionuclide purity," Journal of the Physical Society of Japan, vol. 2022, pp. 1–10.

[33]. K. Kossert et al., "Activity determination and nuclear decay data of 177Lu," Applied Radiation and Isotopes, vol. 70, pp. 2215–2221, 2012.

[34]. S. Banerjee, M. R. A. Pillai, and F. F. Knapp, "Lutetium-177 therapeutic radiopharmaceuticals: Linking chemistry, radiochemistry, and practical applications," Chemical Reviews, vol. 115, pp. 2934–2974, 2015.

[35]. M. R. A. Pillai et al., "Production logistics of 177Lu for radionuclide therapy," Applied Radiation and Isotopes, vol. 59, pp. 109–118, 2003.

[36]. L. Rosmayani et al., "Simulation of irradiation calculations on lutetium-177 production in RSG-GAS using U3Si2-Al and U9Mo-Al fuels," Jurnal Teknologi Reaktor Nuklir Tri Dasa Mega, vol. 25, p. 45, 2023.

[37]. Maskur et al., "Development of polyethylene glycol-modified gold nanoparticles for the delivery of lutetium-177 radiopharmaceuticals based on antibodies," Journal of Drug Delivery Science and Technology, vol. 100, p. 106104, 2024.

[38]. M. Bé, V. Chisté, and C. Dulieu, Table of Radionuclides, vol. 2. BIPM, 2004, pp. 106–112.

[39]. Y. Yang et al., "Whole process establishment of carrier-free 177Lu production: From small-scale production to pilot-scale production," Journal of Radioanalytical and Nuclear Chemistry, vol. 332, pp. 4917–4928, 2023.

 DOI: https://doi.org/10.55981/urania.2026.13640